

# Impacts of atmospheric ultrafast Kelvin waves on radio scintillations in the equatorial ionosphere

Guiping Liu,<sup>1</sup> Thomas J. Immel,<sup>1</sup> Scott L. England,<sup>1</sup> Harald U. Frey,<sup>1</sup>  
Stephen B. Mende,<sup>1</sup> Karanam K. Kumar,<sup>2</sup> and Geetha Ramkumar<sup>2</sup>

Received 5 September 2012; revised 16 January 2013; accepted 17 January 2013.

[1] We present a statistical analysis of the amplitudes of GPS scintillations (S4 index) observed throughout 2008–2010 using the satellite radio occultation measurements of the Constellation Observing System for Meteorology, Ionosphere, and Climate (COSMIC). Here, for the first time, periodic variability in the occurrence of S4 is investigated using these data. Significant variations of S4 with periods of 2.5–4 days (quasi-3 days) are identified from the observations during postsunset hours (1900–2400 local time) between 15°S–15°N magnetic latitude during this 3 year interval. Coherence analyses of these variations with the geomagnetic Ap index, solar EUV irradiance, and atmospheric wind measurements from an equatorial mesosphere meteor radar at Thumba, India (8.5°N, 77°E) are performed, providing a measure of the relationship between variations in the scintillations and potential drivers. The quasi-3 day variations in S4 are found to covary with the variations of the three drivers examined. In particular, the S4 signatures are found to be coherent with the atmospheric ultrafast Kelvin (UFK) planetary waves characterized by the zonal wind measurements of the radar. This study shows that these UKF waves are as important as the solar and geomagnetic drivers in forcing the day-to-day variations of the occurrence of equatorial spread *F*.

**Citation:** Liu, G., T. J. Immel, S. L. England, H. U. Frey, S. B. Mende, K. K. Kumar, and G. Ramkumar, Impacts of atmospheric ultrafast Kelvin waves on radio scintillations in the equatorial ionosphere (2013), *J. Geophys. Res. Space Physics*, 118, doi:10.1002/jgra.50139.

## 1. Introduction

[2] Radio signals transmitted from GPS satellites to receivers can suffer fluctuations in both amplitude and phase due to the presence of small-scale irregularities in electron density in the ionosphere [e.g., Basu *et al.*, 1988; Aarons, 1993; Anderson *et al.*, 2004]. These fluctuations, termed radio scintillations, may induce errors or loss in access to satellite-based communication and navigation systems [Basu *et al.*, 2002]. Because of this, the occurrence of scintillations has been studied extensively and has known dependence on latitude, longitude, season, and local time [e.g., Aarons, 1993; Basu *et al.*, 2002; Anderson *et al.*, 2004]. However, the scintillation occurrence has a large variability and is thus difficult to predict. Here we report a study of the day-to-day occurrence of such scintillations.

[3] Radio scintillations are produced by small-scale electron density irregularities often occurring along with

large-scale *F* region irregularities in the equatorial region, called equatorial spread *F* (ESF) [Basu *et al.*, 1988]. The generation of ESF is affected by processes including the prereversal enhancement of  $E \times B$  upward drifts driven by evening conductivity gradients and *F* region neutral winds [e.g., Fejer *et al.*, 1999; Takahashi *et al.*, 2005; Abdu *et al.*, 2006; Fagundes *et al.*, 2009]. Additionally, the strength of the *E* region neutral wind dynamo [e.g., Heelis *et al.*, 1974] that drives the growth of the daytime equatorial ionosphere can modulate the density of the ionospheric *F* peak and so may also affect the occurrence of ESF and scintillations.

[4] Both solar and geomagnetic forcing are known to have impacts on the ionosphere that could affect the occurrence of ESF. In terms of the solar forcing, the occurrence of ESF has been observed to depend on solar EUV irradiance [e.g., Su *et al.*, 2009; Heelis *et al.*, 2010]. Regarding the geomagnetic forcing, penetrating electric fields from the magnetosphere and disturbance dynamo fields originating from auroral heating could produce upward drifts at the equator, affecting plasma densities and thereby changing the probability of ESF occurrence [e.g., Batista *et al.*, 1986; Fejer and Scherliess, 1997; Burke *et al.*, 2009; Heelis *et al.*, 2010].

[5] Scintillation occurrence has been found to exhibit a large day-to-day variability that is still not understood [e.g., Anderson *et al.*, 2004; Basu *et al.*, 2009],

<sup>1</sup>Space Sciences Laboratory, University of California, Berkeley, California, USA.

<sup>2</sup>Space Physics Laboratory, Vikram Sarabhai Space Center, Trivandrum, 695022, India.

Corresponding author: G. Liu, Space Sciences Laboratory, University of California, Berkeley, CA, 94720, USA. (guiping@ssl.berkeley.edu)

©2013. American Geophysical Union. All Rights Reserved.  
2169-9380/13/10.1002/jgra.50139

although likely linked in part to the variation in  $F$ -layer density, and in part to the intensity of the prereversal enhancement. Since each of these are related to conditions in the neutral atmosphere, as well as geomagnetic and solar EUV drivers, this study investigates the day-to-day variability of these scintillations by examining the relationship between periodic variations in the upper atmosphere, geomagnetic and solar forcing indices, and the S4 index.

[6] The neutral atmosphere wind velocity can be modulated by planetary-scale waves with periods of a few days [e.g., *Andrews et al.*, 1987]. Some planetary waves may propagate into the  $E$  region [e.g., *Forbes*, 2000; *Takahashi et al.*, 2007], and the changes in neutral winds that they may introduce produce concomitant changes in the dynamo electric fields [e.g., *Heelis et al.*, 1974]. These fields are transmitted to the  $F$  region along magnetic field lines so that the effects of atmospheric planetary waves may be extended into higher altitudes of the ionosphere. Some planetary waves are confined to lower altitudes below the  $E$  region, but their influences can be carried into higher altitudes via an intermediary such as tides [e.g., *Lastovicka*, 2006; *Liu et al.*, 2010a]. Having been affected by planetary waves, these tides may then modulate the  $E$  region dynamo and, hence,  $\mathbf{E} \times \mathbf{B}$  drifts and densities in the ionosphere. Correspondences between the day-to-day changes of the ionosphere with periods of 2–30 days and the occurrences of atmospheric planetary waves have been reported [e.g., *Laštovička*, 2006; *Pancheva et al.*, 2006; *Pedatella and Forbes*, 2009; *Liu et al.*, 2010a, 2010b, 2012; *England et al.*, 2012].

[7] Ultrafast Kelvin (UFK) waves are one type of atmospheric planetary wave that may propagate upward into the mesosphere or even higher into the thermosphere, depending on factors such as the background atmospheric conditions or the vertical wavelengths of the waves [e.g., *Forbes*, 2000; *Takahashi et al.*, 2007]. These waves have periods of 2.5 to 4 days and are trapped at low latitudes [*Salby and Garcia*, 1987]. They can directly modulate the dynamo and change the conductivity at sunset that controls the prereversal enhancement, so they can affect the formation of ESF [e.g., *Takahashi et al.*, 2005; *Abdu et al.*, 2006]. Therefore, UKF waves are of potential importance for producing the day-to-day variability in the occurrence of equatorial scintillations.

[8] Previous studies have found cases when periodic variations of  $\mathbf{E} \times \mathbf{B}$  upward drifts and ESF in the ionosphere are present simultaneously with atmospheric planetary waves observed in the neutral wind velocity measurements of the atmosphere [e.g., *Takahashi et al.*, 2005; *Abdu et al.*, 2006; *Fagundes et al.*, 2009]. In this study, we perform a statistical survey of the 2.5–4 day (quasi-3 day) variations of the amplitudes of scintillations (S4 index) in the equatorial ionosphere in relation to UKF waves using the available S4 observations of the satellite radio occultation measurements by the Constellation Observing System for Meteorology, Ionosphere, and Climate (COSMIC) for three continuous years from 2008 to 2010. Because the 2–4 day planetary wave signatures in the ionosphere have been observed to be coherent between stations separated by up to  $80^\circ$  longitude [e.g., *Altadill and Apostolov*, 2003; *Laštovička et al.*, 2006], the COSMIC S4 data over a correspondingly large geographic area can be combined.

The zonal wind measurements by the SKiYMET meteor radar at Thumba, India ( $8.5^\circ\text{N}$ ,  $77^\circ\text{E}$ ) at the magnetic equator are used to characterize the quasi-3 day UKF waves in the mesosphere based upon their periods and vertical propagation properties. These waves identified are found to covary with the quasi-3 day variations in S4 at various time intervals through 3 years, showing a connection between the day-to-day occurrences of scintillations and the atmospheric UKF waves. A similar analysis is also performed with the solar and geomagnetic drivers, and their relationships to the scintillation day-to-day occurrences are compared with the UKF waves.

## 2. Data and Analysis

[9] The COSMIC six-satellite constellation measures the ionosphere through GPS radio occultations (the measurements are made all about the globe with  $\sim 2000$  occultations each day) [*Schreiner et al.*, 2007]. Since late 2007, the satellites are evenly spaced into orbits with orbital planes separated by  $24^\circ$  longitude at  $72^\circ$  inclination and  $\sim 800$  km altitude. These observations cover an extended period of time, and the data for the 3 years from 2008 to 2010 are used in this study to perform a statistical analysis.

[10] COSMIC can directly measure the scintillation amplitude during each occultation using the GPS L1 channel at 1.5 GHz. Each occultation normally lasts 1–15 min, depending on the viewing geometry [*Dymond*, 2012]. The S4 index (the standard deviation of signal power divided by the mean power) has been derived and is provided as a processed data product by the COSMIC Data Analysis and Archive Center (CDAAC). These data are provided at 1 s time intervals during each occultation, and the average value over 9 s time around the observed maximum S4 has been calculated. This averaging process removes anomalously high S4 values within very short time intervals and provides an indication of the presence of scintillations [e.g., *Ko and Yeh*, 2010].

[11] This study uses the COSMIC occultation measurements for tangent points between 150 and 800 km altitude and  $\pm 15^\circ$  magnetic latitude. This ensures that only scintillations related to ESF are considered. The S4 index data at local times between 1900 and 2400 h are selected, so only postsunset scintillations are studied. These data are grouped into four bins of geographic longitude (each  $40^\circ$  wide and within  $80^\circ$  longitude of the radar site in India). The S4 measured by COSMIC depends on the satellite viewing geometry, which changes with time and is different for every occurrence of scintillations. ESF are sporadic and may not always be observed by COSMIC. For this reason, the average values of S4 of each day of observations are calculated and used for the analysis in this study.

[12] Figures 1b–1d display the time series of the S4 index on each day for each year from 2008 to 2010 over the Indian sector at  $40^\circ$ – $80^\circ$  geographic longitude and  $15^\circ\text{S}$ – $15^\circ\text{N}$  magnetic latitude (this region is highlighted in Figure 1a). Figure 1 shows that the S4 values are almost continuous throughout the time period. A wavelet analysis can be applied to the time series of the COSMIC S4 to identify any periodic variation. Such an analysis has been applied successfully in atmospheric and ionospheric studies [e.g., *Takahashi et al.*, 2005; *Laštovička et al.*, 2006],

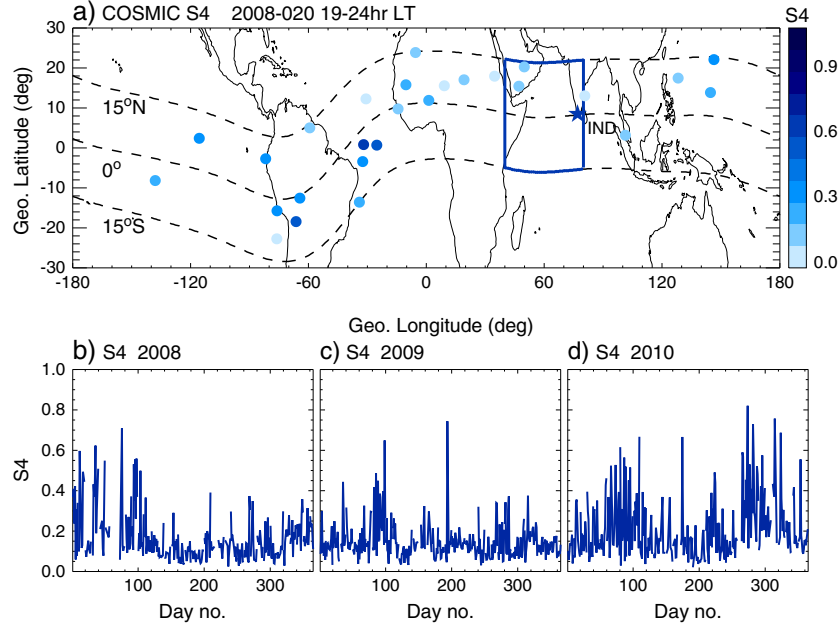


**Figure 1.** (a) Blue circles represent the S4 scintillation index measurements by COSMIC at 15°S–15°N magnetic latitude in the local time range of 1900–2400 h on 20 January 2008. The blue box highlights the Indian sector at 15°S–15°N magnetic latitude and 40°–80°E geographic longitude for which the results of the analysis are shown in this study. The blue star marks the location of the meteor radar at Thumba, India (8.5°N, 77°E). The black dashed lines represent the ±15° magnetic latitudes and the magnetic equator. (b–d) Time series of the COSMIC S4 data over the Indian sector for individual years of 2008, 2009, and 2010, respectively.

decomposing the time series into time-frequency space, so that both the periods of the variations and their occurrences in time are determined.

[13] A wavelet analysis is used to identify quasi-3 day UFK waves in the atmospheric wind observations by the SKiYMET meteor radar at Thumba (8.5°N, 77°E), India. This radar is located at the magnetic equator (see Figure 1a), and it measures neutral winds in the mesosphere at 83–98 km altitude at about 3 km range intervals [Kumar *et al.*, 2007]. Near-continuous measurements are provided for each day throughout the same time period as the COSMIC S4 data from 2008 to 2010. The UFK waves propagate eastward with respect to the background flow, traveling over all longitudes in the equatorial region [Salby and Garcia, 1987]. The wind measurements at this radar site are thus sufficient to characterize these planetary-scale waves. UFK waves are characterized by wind perturbations in the zonal direction [e.g., Andrews *et al.*, 1987], although some nonzero meridional wind components are observed [e.g., Riggan *et al.*, 1997; England *et al.*, 2012]. The zonal wind measurements by this radar for each altitude in the mesosphere are used to search for UFK wave signatures, providing a continuous indication of the occurrence of the UFK waves simultaneous with the scintillation observations.

[14] The same wavelet analysis is applied to the time series of the daily means of solar irradiance of the 30.4 nm Helium-II solar EUV line, as measured by the Solar EUV Experiment (SEE) on the TIMED satellite mission, and the Ap indices to investigate the impacts of the solar and geomagnetic activities on the occurrence of scintillations. Quasi-3 day variation signatures are identified from these

observations, and their correspondences with the S4 variations are presented. The role of these solar and geomagnetic drivers on the S4 day-to-day variations is then compared to that of the atmospheric UFK waves.

### 3. Results

[15] Figures 2a–2d give the wavelet power spectra of the time series of the COSMIC S4 over the Indian sector, the Ap, the solar EUV irradiance, and the atmospheric zonal wind measurements at 98 km altitude throughout 2008–2010. The spectra indicate that there are significant (at the 95% confidence level) variations having periods between 2.5 and 4 days (quasi-3 days) present in all series. Variations with periods of 5–8 days are also observed, but they are not considered because this study focuses on the quasi-3 day waves.

[16] The wavelet coherence (i.e., a localized correlation coefficient in time-frequency space between two time series [e.g., Grinsted *et al.*, 2004]) is now calculated to examine the relationship of the scintillation variations with the various possible drivers. The wavelet coherence analysis presented in Figures 3a–3c gives the calculated correlation coefficient between S4 and Ap, solar irradiance, and atmospheric wind, respectively. Large values of coherence ( $\geq 0.9$ ) are seen for 2.5–4 day periods at many different times. A simplified illustration of these correlations is provided later.

[17] The atmospheric wind measurements are also used to diagnose the observed quasi-3 day waves are in fact the upward propagating UFK waves. Figure 4 gives an

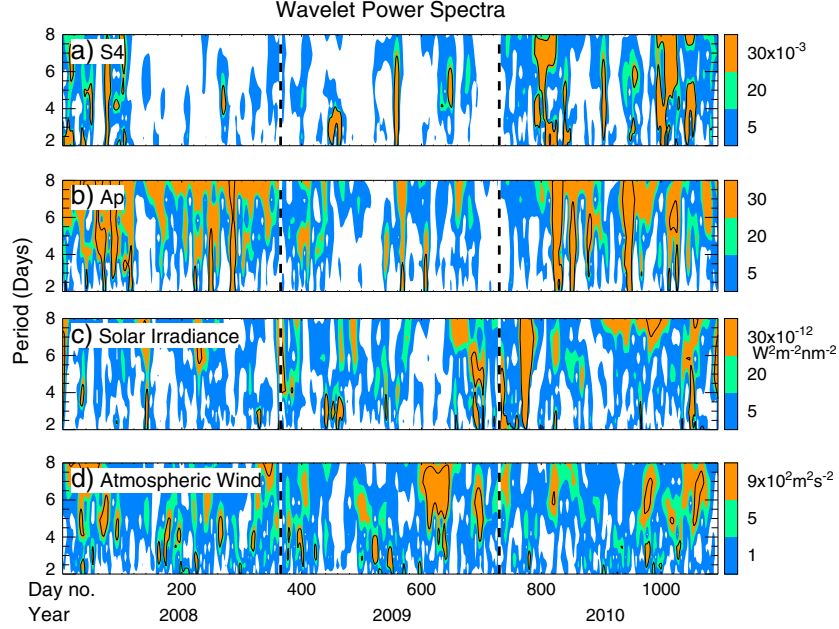


**Figure 2.** The wavelet power spectra for (a) the COSMIC S4 data over India, (b) Ap index, (c) solar EUV irradiance measurements by TIMED/SEE, and (d) atmospheric zonal wind measurements by the meteor radar at Thumba. The spectrum is calculated based upon the daily mean values throughout 2008–2010. The black contours indicate regions that are statistically significant (at the 95% confidence level). The dashed lines mark the first days of 2009 and 2010.

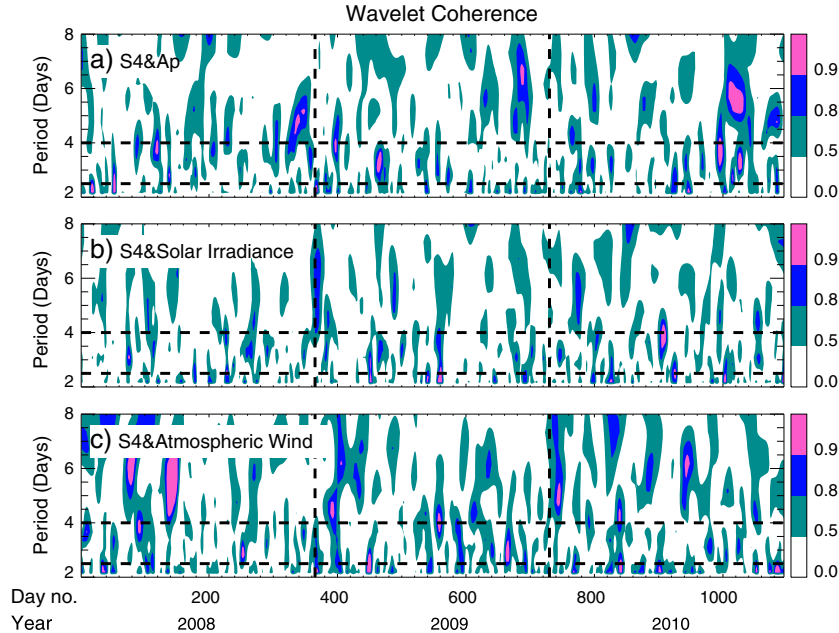


**Figure 3.** The wavelet coherence of (a) between S4 and Ap index, (b) between S4 and solar irradiance, and (c) between S4 and atmospheric wind at Thumba throughout 2008–2010. The contours show the wavelet squared coherence at values of 0.5, 0.8, and 0.9. The horizontal dashed lines mark the 2.5 day and 4 day periods. The vertical dashed lines mark the first days of 2009 and 2010.

example of the calculation of the vertical wavelength for the wave over 1–20 January 2008. Figures 4a–4f show the zonal winds measured at 82–98 km altitude, filtered for 2.5–3.5 day signatures (for this example, the wind wavelet

spectrum peaks at  $\sim 3$  days). Using the crests of the wave at each altitude (shown by the colored dots), it is possible to find the progression of the wave's phase with altitude. The phase of this wave decreases with increasing altitude,

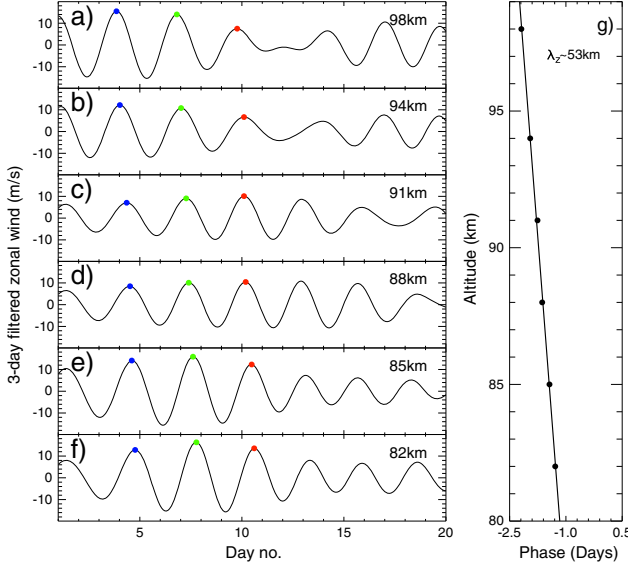


**Figure 4.** (a–f) Amplitude of 2.5–3.5 day filtered zonal winds measured by the SKiYMET radar at Thumba for 82–98 km altitudes over 1–20 January 2008 (day number 1–20). The dots mark the maxima of the winds. (g) Phase of the quasi-3 day wave at different altitudes. The straight line is from the linear regression. The slope of the line indicates the vertical wavelength of this wave to be 44–62 km, assuming uncertainties for the period and least-squares fit.

suggesting the upward propagation of the wave. From the slope of the straight line (shown in Figure 4g), it is possible to find the vertical wavelength of this wave. The vertical wavelength is found to be in the range of 44–62 km, taking into account the uncertainties of the slope and the wave period (2.5–3.5 days).

[18] The determined wavelength agrees with the vertical wavelength of an UFK wave as reported by previous observational studies [e.g., *Forbes*, 2000; *Takahashi et al.*, 2009; *Davis et al.*, 2012]. It also agrees with the theoretical calculation result. From the Kelvin wave dispersion relation [e.g., *Holton et al.*, 2001],

$$\lambda_z = N \left( \frac{\lambda_x}{\tau} - \bar{u} \right) \quad (1)$$

where  $\lambda_z$  is the vertical wavelength,  $\lambda_x$  is the horizontal wavelength,  $N$  is the Brunt-Väisälä period ( $\sim 300$  s),  $\tau$  is the wave period, and  $\bar{u}$  is the zonal mean zonal wind. The vertical wavelength is  $\sim 50$  km for a 3 day zonal wave number-1 Kelvin wave ( $\lambda_x$  is  $\sim 40,000$  km) if we use the value of the mean zonal wind of  $-12.5$  m s $^{-1}$  at 91 km altitude as measured by the SKiYMET radar for  $\bar{u}$ . This provides evidence that this quasi-3 day wave is most likely an UFK wave.

[19] The same calculation is performed for all of the time intervals at which the S4 variations are found to covary with the atmospheric quasi-3 day waves (see Figure 3c). Table 1 lists the calculated vertical wavelengths for the intervals that are characterized of UFK wave signatures. Any interval which does not have a clear wave structure or vertical wavelength is not included. The wavelengths determined from the neutral wind measurements are listed in comparison with the theoretical values. These wavelengths all fall within the

range of vertical wavelengths of UFK waves as reported in previous studies [e.g., *Forbes*, 2000; *Takahashi et al.*, 2009; *Davis et al.*, 2012]. They also agree with the theoretical calculation results according to the Kelvin wave dispersion relation [e.g., *Holton et al.*, 2001]. Therefore, those quasi-3 day waves observed in the neutral wind observations and that covary with the S4 variations are indicative of UFK wave signatures.

[20] Figure 5 includes the days on which the quasi-3 day variations of S4 covary with the variations of Ap, solar EUV irradiance, and UFK waves throughout 2008–2010 for the Indian sector. This figure also provides a comparison between different drivers of scintillation variations. There are nine intervals in which the S4 and Ap variations are coherent and seven other intervals during which the S4 and solar irradiance variations are coherent. Coherence between S4 and atmospheric UFK waves is seen at eight intervals. Thus, coherent variations are seen between S4 and three separate drivers with nearly equal occurrence rates.

[21] The same analysis has been applied at all 4 longitudinal bins within  $80^\circ$  of the meteor radar at Thumba. Correspondences between scintillations and each of possible drivers are summarized in Table 2 for each geographic region. The table shows again that the S4 quasi-3 day variations correlate with the variations of the neutral winds as well as the solar and geomagnetic activities. A total of 24 cases are observed when the S4 variations covary with one of the three possible drivers examined here. On average, the

**Table 1.** Vertical Wavelengths of the Quasi-3 Day Waves Observed in the Neutral Wind Measurements in Comparison with the Theoretical Values of an UFK Wave

Interval Day Number	Wind Measurement		Theoretical Value	
	$\lambda_z$ (km)	$\bar{u}$ (m s $^{-1}$ )	$\lambda_z$ (km)	Wave Number
2–13	44–62	-12.5	50	1
89–102	49–69	-16.9	51	1
248–255	24–34	-11.6	27	2
445–452	18–25	-13.7	27	2
554–560	41–49	24.1	39	1
637–642	35–50	-29.6	55	1
660–668	43–60	12.6	43	1
835–842	28–40	31.4	37	1
583–595	40–56	-18.8	52	1

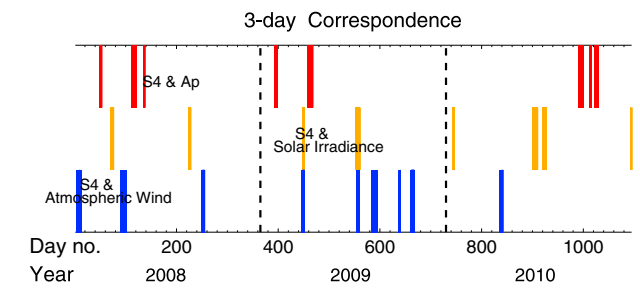


**Figure 5.** The colored bars mark the time intervals at which the 2.5–4 day variations are coherent (coherence  $\geq 0.9$ ) between S4 and Ap index (red bars), S4 and solar irradiance (yellow bars), and S4 and atmospheric UFK waves (blue bars). The adjacent days that the wavelet coherence is greater than 0.8 are also included.

**Table 2.** Total Number of Correspondences of Quasi-3 Day Variations Between S4 and Various Drivers During 2008–2010 for Different Geographic Longitudinal Sectors

Sector	Longitude (deg)	S4 and <i>Ap</i>	S4 and Solar Irradiance	S4 and Neutral Wind
1	0–40	9	6	6
2	40–80	8	8	9
3	80–120	4	8	11
4	120–160	16	7	6
	mean	9	7	8

quasi-3 day variations in S4 are correlated with those in *Ap* for 9 of 24 cases ( $\sim 38\%$ ), they covary with the variations in solar irradiance for 7 of 24 cases ( $\sim 29\%$ ), and they covary with the atmospheric waves for 8 of 24 cases ( $\sim 33\%$ ). The atmospheric UFK waves appear to be as important as the solar and geomagnetic drivers in forcing the day-to-day variations in S4.

#### 4. Summary and Conclusions

[22] We have presented a detailed examination of the occurrence of quasi-3 day variations of the amplitudes of scintillations in the equatorial ionosphere in relation to atmospheric, solar, and geomagnetic forcing. The S4 index observations from the COSMIC/GPS radio occultation measurements at postsunset hours (1900–2400 LT) and  $15^{\circ}\text{S}$ – $15^{\circ}\text{N}$  magnetic latitude exhibit significant (above the 95% statistical confidence level) quasi-3 day variations during the 3 years of 2008–2010. These S4 variations are shown to covary with corresponding variations in the *Ap* index, solar EUV irradiance, and atmospheric wind measurements at different times (on average 38% of the S4 variations correlate to the *Ap* variations, 29% of them correlate to the solar irradiance, and 33% of them correlate to the neutral wind variations). These correspondences are seen over a  $80^{\circ}$  longitude geographic area, indicating a large-scale signature. This is the first time that periodic variation signatures of scintillations are studied using the satellite S4 index data of COSMIC throughout an extended time period (3 years).

[23] The quasi-3 day waves in the atmosphere are identified from the mesospheric zonal wind measurements by a SKiYMET meteor radar at the magnetic equator. These waves are most likely UFK planetary waves that have periods of 3–4 days and exist in the equatorial region [e.g., *Salby and Garcia*, 1987]. An examination of the vertical wavelengths of these waves supports that they are of UFK wave signatures. These waves are found at many time intervals to covary with the scintillation variations in the equatorial ionosphere. This study presents evidence of the UFK wave signatures in S4 using a statistical analysis of 3 years of observations.

[24] The quasi-3 day waves occur on many occasions throughout the 3 years. Occurrences of these waves correspond to the variations in S4 at many time intervals, and these correspondences are observed as often as those between S4 and the solar and geomagnetic drivers. This study shows that the atmospheric driver is comparable to the solar and geomagnetic drivers in forcing the S4 3 day

variations. The atmospheric quasi-3 day planetary waves should be taken into account in interpreting the day-to-day variability of ESF and scintillations.

[25] **Acknowledgments.** This research work was supported by NASA's Heliophysics Research program through Award number NNX12AD48G and Living With a Star program through Award number NNX11APO4G. The S4 data are obtained from the COSMIC Data Analysis and Archive Center (CDAAC). The *Ap* index data are obtained from the World Data Center for Geomagnetism, Kyoto. The TIMED/SEE solar irradiance data are available at <http://lasp.colorado.edu>.

#### References

Aarons, J. (1993), The longitudinal morphology of equatorial *F*-layer irregularities relevant to their occurrence, *Space Sci. Rev.*, *63*, 209–243, doi: 10.1007/BF00750769.

Abdu, M. A., P. P. Batista, I. S. Batista, C. G. M. Brum, A. J. Carrasco, and B. W. Reinisch (2006), Planetary wave oscillations in mesospheric winds, equatorial evening prereversal electric field and spread *F*, *Geophys. Res. Lett.*, *33*, L07107, doi: 10.1029/2005GL024837.

Altadill, D., and E. M. Apostolov (2003), Time and scale size of planetary wave signatures in the ionospheric *F* region: Role of the geomagnetic activity and mesosphere/lower thermosphere winds, *J. Geophys. Res. Space Phys.*, *108*, 1403, doi: 10.1029/2003JA010015.

Anderson, D. N., B. Reinisch, C. Valladare, J. Chau, and O. Veliz (2004), Forecasting the occurrence of ionospheric scintillation activity in the equatorial ionosphere on a day-to-day basis, *J. Atmos. Sol. Terr. Phys.*, *66*, 1567–1572, doi: 10.1016/j.jastp.2004.07.010.

Andrews, D. A., J. R. Holton, and C. B. Leovy (1987), *Middle Atmosphere Dynamics*, 202–206, Academic Press, San Diego.

Basu, S., E. MacKenzie, and S. Basu (1988), Ionospheric constraints on VHF/UHF communications links during solar maximum and minimum periods, *Radio Sci.*, *23*, 363–378, doi: 10.1029/RS023i003p00363.

Basu, S., K. M. Groves, S. Basu, and P. J. Sultan (2002), Specification and forecasting of scintillations in communication/navigation links: Current status and future plans, *J. Atmos. Sol. Terr. Phys.*, *64*, 1745–1754, doi: 10.1016/S1364-6826(02)00124-4.

Basu, S., S. Basu, J. Huba, J. Krall, S. E. McDonald, J. J. Makela, E. S. Miller, S. Ray, and K. Groves (2009), Day-to-day variability of the equatorial ionization anomaly and scintillations at dusk observed by GUVI and modeling by SAMI3, *J. Geophys. Res. Space Phys.*, *114*, A04302, doi: 10.1029/2008JA013899.

Batista, I. S., M. A. Abdu, and J. A. Bittencourt (1986), Equatorial *F* region vertical plasma drifts—Seasonal and longitudinal asymmetries in the American sector, *J. Geophys. Res.*, *91*, 12,055–12,064, doi: 10.1029/JA091iA11p12055.

Burke, W. J., O de La Beaujardière, L. C. Gentile, D. E. Hunton, R. F. Pfaff, P. A. Roddy, Y.-J. Su, and G. R. Wilson (2009), C/NOFS observations of plasma density and electric field irregularities at post-midnight local times, *Geophys. Res. Lett.*, *36*, L00C09, doi: 10.1029/2009GL038879.

Davis, R. N., Y.-W. Chen, S. Miyahara, and N. J. Mitchell (2012), The climatology, propagation and excitation of ultra-fast Kelvin waves as observed by meteor radar, Aura MLS, TRMM and in the Kyushu-GCM, *Atmospheric Chemistry & Physics*, *12*, 1865–1879, doi: 10.5194/acp-12-1865-2012.

Dymond, K. (2012), Global observations of L band scintillation at solar minimum made by COSMIC, *Radio Sci.*, *47*, RS0L18, doi: 10.1029/2011RS004931.

England, S. L., G. Liu, Q. Zhou, T. J. Immel, K. K. Kumar, and G. Ramkumar (2012), On the signature of the quasi-three-day wave in the thermosphere during the January 2010 URSI World Day Campaign, *J. Geophys. Res.*, *117*, A06304, doi: 10.1029/2012JA017558.

Fagundes, P. R., J. A. Bittencourt, J. R. Abalde, Y. Sahai, M. J. A. Bolzan, V. G. Pillat, and W. L. C. Lima (2009), *F* layer postsunset height rise due to electric field prereversal enhancement: 1. Traveling planetary wave ionospheric disturbance effects, *J. Geophys. Res. Space Phys.*, *114*, A12321, doi: 10.1029/2009JA014390.

Fejer, B. G., and L. Scherliess (1997), Empirical models of storm time equatorial zonal electric fields, *J. Geophys. Res.*, *102*, 24,047–24,056, doi: 10.1029/97JA02164.

Fejer, B. G., L. Scherliess, and E. R. de Paula (1999), Effects of the vertical plasma drift velocity on the generation and evolution of equatorial spread *F*, *J. Geophys. Res.*, *104*, 19,859–19,870, doi: 10.1029/1999JA900271.

Forbes, J. M. (2000), Wave coupling between the lower and upper atmosphere: Case study of an ultra-fast Kelvin Wave, *J. Atmos. Sol. Terr. Phys.*, *62*, 1603–1621, doi: 10.1016/S1364-6826(00)00115-2.

Grinsted, A., J. C. Moore, and S. Jevrejeva (2004), Application of the cross wavelet transform and wavelet coherence to geophysical time series, *Nonlinear Process Geophys.*, **11**, 561–566.

Heelis, R. A., P. C. Kendall, R. J. Moffett, D. W. Windle, and H. Rishbeth (1974), Electrical coupling of the *E*- and *F*-regions and its effect on *F*-region drifts and winds, *Planet Space Sci.*, **22**, 743–756, doi: 10.1016/0032-0633(74)90144-5.

Heelis, R. A., R. Stoneback, G. D. Earle, R. A. Haaser, and M. A. Abdu (2010), Medium-scale equatorial plasma irregularities observed by coupled ion-neutral dynamics investigation sensors aboard the communication navigation outage forecast system in a prolonged solar minimum, *J. Geophys. Res. Space Phys.*, **115**, A10321, doi: 10.1029/2010JA015596.

Holton, J. R., M. J. Alexander, and M. T. Boehm (2001), Evidence for short vertical wavelength Kelvin waves in the department of energy-atmospheric radiation measurement Nauru99 radiosonde data, *J. Geophys. Res.*, **106**, 20,125–20,130, doi: 10.1029/2001JD900108.

Ko, C. P., and H. C. Yeh (2010), COSMIC/FORMOSAT-3 observations of equatorial *F* region irregularities in the SAA longitude sector, *J. Geophys. Res. Space Phys.*, **115**, A11309, doi: 10.1029/2010JA015618.

Kumar, K. K., G. Ramkumar, and S. T. Shelbi (2007), Initial results from SKiYMET meteor radar at Thumba (8.5°N, 77°E): 1. Comparison of wind measurements with MF spaced antenna radar system, *Radio Sci.*, **42**, RS6008, doi: 10.1029/2006RS003551.

Laštovička, J. (2006), Forcing of the ionosphere by waves from below, *J. Atmos. Sol. Terr. Phys.*, **68**, 479–497, doi: 10.1016/j.jastp.2005.01.018.

Laštovička, J., P. Šauli, and P. Križan (2006), Persistence of planetary wave type oscillations in the mid-latitude ionosphere, *Ann. Geophys.*, **49**, 1189–1200.

Liu, G., T. J. Immel, S. L. England, K. K. Kumar, and G. Ramkumar (2010a), Temporal modulations of the longitudinal structure in *F*<sub>2</sub> peak height in the equatorial ionosphere as observed by COSMIC, *J. Geophys. Res. Space Phys.*, **115**, A04,303, doi: 10.1029/2009JA014829.

Liu, G., T. J. Immel, S. L. England, K. K. Kumar, and G. Ramkumar (2010b), Temporal modulation of the four-peaked longitudinal structure of the equatorial ionosphere by the 2 day planetary wave, *J. Geophys. Res. Space Phys.*, **115**, A12,338, doi: 10.1029/2010JA016071.

Liu, G., S. L. England, T. J. Immel, K. K. Kumar, G. Ramkumar, and L. P. Goncharenko (2012), Signatures of the 3-day wave in the low- and mid-latitude ionosphere during the January 2010 URSI World Day campaign, *J. Geophys. Res. Space Phys.*, **117**, A06305, doi: 10.1029/2012JA017588.

Pancheva, D. V., et al. (2006), Two-day wave coupling of the low-latitude atmosphere-ionosphere system, *J. Geophys. Res. Space Phys.*, **111**, A07313, doi: 10.1029/2005JA011562.

Pedatella, N. M., and J. M. Forbes (2009), Modulation of the equatorial *F*-region by the quasi-16-day planetary wave, *Geophys. Res. Lett.*, **360**, L09105, doi: 10.1029/2009GL037809.

Riggin, D. M., D. C. Fritts, T. Tsuda, T. Nakamura, and R. A. Vincent (1997), Radar observations of a 3-day Kelvin wave in the equatorial mesosphere, *J. Geophys. Res.*, **102**, 26,141–26,158, doi: 10.1029/96JD04011.

Salby, M. L., and R. R. Garcia (1987), Transient response to localized episodic heating in the tropics. Part I: Excitation and short-time near-field behavior, *J. Atmos. Sci.*, **44**, 458–498, doi: 10.1175/1520-0469(1987)044<0458:TRTLEH>2.0.CO;2.

Schreiner, W., C. Rocken, S. Sokolovskiy, S. Syndergaard, and D. Hunt (2007), Estimates of the precision of GPS radio occultations from the COSMIC/FORMOSAT-3 mission, *Geophys. Res. Lett.*, **34**, L04808, doi: 10.1029/2006GL027557.

Su, S.-Y., C. K. Chao, and C. H. Liu (2009), Cause of different local time distribution in the postsunset equatorial ionospheric irregularity occurrences between June and December solstices, *J. Geophys. Res. Space Phys.*, **114**, A04321, doi: 10.1029/2008JA013858.

Takahashi, H., L. M. Lima, C. M. Wrassse, M. A. Abdu, I. S. Batista, D. Gobbi, R. A. Buriti, and P. P. Batista (2005), Evidence on 2–4 day oscillations of the equatorial ionosphere *h'*<sub>F</sub> and mesospheric airglow emissions, *Geophys. Res. Lett.*, **32**, L12102, doi: 10.1029/2004GL022318.

Takahashi, H., et al. (2007), Signatures of ultra fast Kelvin waves in the equatorial middle atmosphere and ionosphere, *Geophys. Res. Lett.*, **34**, L11108, doi: 10.1029/2007GL029612.

Takahashi, H., et al. (2009), Possible influence of ultra-fast Kelvin wave on the equatorial ionosphere evening uplifting, *Earth, Planets, and Space*, **61**, 455–462.